Towards Area-Based In Vitro Metabolic Engineering: Assembly of Pfs Enzyme onto Patterned Microfabricated Chips

Angela T. Lewandowski
Dept. of Chemical and Biomolecular Engineering, University of Maryland, College Park, MD 20742

William E. Bentley
Dept. of Chemical and Biomolecular Engineering, University of Maryland, College Park, MD 20742
Center for Biosystems Research, University of Maryland Biotechnology Institute, College Park, MD 20742
Fischell Dept. of Bioengineering, University of Maryland, College Park, MD 20742

Hyunmin Yi
Dept. of Materials Science and Engineering, University of Maryland, College Park, MD 20742

Gary W. Rubloff
Dept. of Materials Science and Engineering, University of Maryland, College Park, MD 20742
Institute for Systems Research, University of Maryland, College Park, MD 20742
Institute for Research in Electronics and Applied Physics, University of Maryland, College Park, MD 20742

Gregory F. Payne
Center for Biosystems Research, University of Maryland Biotechnology Institute, College Park, MD 20742

Reza Ghodssi
Institute for Systems Research, University of Maryland, College Park, MD 20742
Dept. of Electrical and Computer Engineering, University of Maryland, College Park, MD 20742

DOI 10.1021/bp.44
Published online September 17, 2008 in Wiley InterScience (www.interscience.wiley.com).

We report an approach for spatially selective assembly of an enzyme onto selected patterns of microfabricated chips. Our approach is based on electrodeposition of the aminopolysaccharide chitosan onto selected electrode patterns and covalent conjugation of a target enzyme to chitosan upon biochemical activation of a genetically fused "pro-tag." We report assembly of S-adenosylhomocysteine nucleosidase (Pfs) fused with a C-terminal pentatyrosine pro-tag. Pfs is a member of the bacterial autoinducer-2 biosynthesis pathway, catalyzing the irreversible cleavage of S-adenosylhomocysteine. The assembled Pfs retains its catalytic activity and structure, as demonstrated by retained antibody recognition. Assembly is controlled by the electrode area, resulting in reproducible rates of catalytic conversion for a given area, and thus allowing for area-based manipulation of catalysis and small molecule biosynthesis. Our approach enables optimization of small molecule biosynthesis in 1-step as well as multistep enzymatic reactions, including entire metabolic pathways, and we envision a wide variety of potential applications.
Keywords: S-adenosylhomocysteine nucleosidase, enzyme assembly, enzyme immobilization, pro-tag, chitosan

Introduction

Integrating biomolecules with microdevices is important but remains challenging because of the labile nature of biomolecules. For example, proteins can lose activity upon immobilization because of unfolding processes.[1] Surface-assembly of catalytically active enzymes remains particularly challenging. To enhance biocompatibility, researchers have created polymer interfaces between the enzymes and the device surfaces.[2–9] The next generation of "smart" biomaterials will require the intimate coupling of advances in microfabrication and biomolecular recognition. The novelty of the approach described here is the use of patterned microdevices (conductive surface patterning) for the assembly of enzymes through an activatable "pro-tag."

Additional Supporting Information may be found in the online version of this article.

Current address of Hyunmin Yi: Department of Chemical and Biological Engineering, Tufts University, Medford, Massachusetts 02155
Correspondence concerning this article should be addressed to W. E. Bentley at bentley@eng.umd.edu.

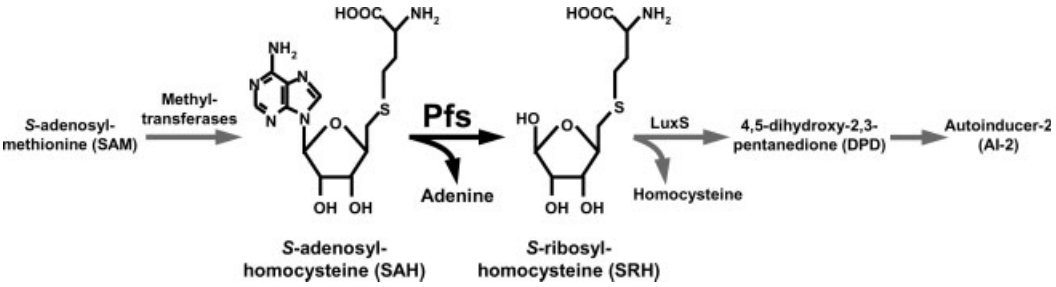

Scheme 1. Pfs irreversibly cleaves SAH into adenine and SRH in the bacterial quorum sensing autoinducer-2 biosynthesis pathway.

Our approach is based on two strategies: (1) electrodeposition of chitosan onto an electrode surface of the microfabricated device, and (2) covalent conjugation of the target enzyme to chitosan upon biochemical activation of a genetically fused pro-tag. First, the aminopolysaccharide chitosan electrodeposits as a stable thin film onto an electrode surface due to its pH-responsive properties conferred by its amine groups. At low pH, the amine groups are protonated, and chitosan is a water-soluble cationic polyelectrolyte. At pH above its *p*Ka (>6.3), the amine groups become deprotonated, and chitosan becomes an insoluble hydrogel network. Because of its pH-responsive properties, chitosan electrodeposits onto a negatively biased electrode surface where local high pH is created.[10–16] Second, tyrosinase activates accessible tyrosine residues of the C-terminal pentatyrosine pro-tag into reactive *o*-quinones, which then covalently link to the nucleophilic amine groups of chitosan to form the protein-chitosan conjugate.[16–20] Chitosan confers its pH-responsive properties to the protein upon covalent conjugation.

We report, for the first time, device-driven assembly of the enzyme Pfs (*S*-adenosylhomocysteine/5′-methylthioadenosine nucleosidase) fused with a C-terminal pentatyrosine pro-tag. As shown in Scheme 1, Pfs is a member of the synthesis pathway for a "universal" signaling molecule in bacterial quorum sensing (autoinducer-2, AI-2) that mediates interspecies cell–cell communication. In this pathway, *S*-adenosylmethionine (SAM) is first converted to *S*-adenosylhomocysteine (SAH) by methyltransferases. Next, Pfs catalyzes the irreversible cleavage of SAH into adenine and *S*-ribosylhomocysteine (SRH).[21] SRH is then converted by the enzyme LuxS (*S*-ribosylhomocysteinase) into homocysteine and 4,5-dihydroxy-2,3-pentanedione, which then goes through several nonenzymatic rearrangements to become AI-2.[22] In addition to quorum sensing, Pfs is involved in important cellular processes, such as protein and DNA methylation and metabolism and polyamine biosynthesis.[23–26] The involvement of Pfs in important bacterial processes makes it an appealing target for the design of new antibiotics. Importantly for antibiotic design, mammalian cells, in contrast, utilize the enzyme SAH hydrolase, which cleaves SAH into homocysteine and adenosine.[27] For this, several researchers have designed inhibitors of Pfs activity as possible antibiotics, and such research is ongoing.[28–31] Thus, assembling Pfs for the controlled examination of its catalytic activity could be used to screen Pfs inhibitors with antibiotic capabilities.

As shown in Scheme 2, Pfs can be assembled by covalent conjugation to chitosan followed by electrodeposition of Pfs-chitosan conjugate onto a patterned electrode (Scheme 2a), or by electrodeposition of chitosan scaffold onto a patterned electrode followed by covalent conjugation of Pfs to the patterned scaffold (Scheme 2b). The procedural order of assembly can be chosen to suit the specific application, demonstrating the versatility of our overall assembly approach. As shown in Scheme 2, the assembled Pfs is recognized through the binding of antibodies, and retains biocatalytic activity, converting SAH substrate into SRH and adenine. The assembly of Pfs is controlled by the electrode patterned area, resulting in reproducible rates of SAH catalytic conversion for a given area and SAH concentration. Correspondingly, using traditional enzyme reaction kinetic models (e.g., Michaelis-Menten) we can "design" specific reaction conditions based on electrode surface area. Furthermore, this control allows for area-based manipulation of the rate of biocatalysis and small molecule biosynthesis, thus enabling optimization of biosynthesis in 1-step as well as the potential for multistep enzymatic reactions. We envision in vitro metabolic engineering applications, based on optimizing catalysis of entire metabolic pathways.

Materials and Methods

Materials

S-adenosylhomocysteine (SAH), bovine serum albumin (BSA), chitosan (minimum 85 % deacetylated chitin; molecular weight 200,000 g/mol) from crab shells, goat anti-mouse IgG conjugated to fluorescein isothiocyanate (FITC), imidazole, isopropyl β-D-thiogalactopyranoside (IPTG), mouse anti-poly-histidine, nickel sulfate, phosphate buffered saline (PBS) (2.7 mM KCl, 137 mM NaCl, 1.5 mM KH_2PO_4, 8.1 mM Na_2HPO_4, pH 7.5), sodium cyanoborohydride, and tyrosinase from mushroom were purchased from Sigma (St. Louis, MO). Tyrosinase was reported by the manufacturer to have an activity of 1,530 U/mg solid. LB (Luria broth) medium was purchased from Becton Dickinson (Cockeysville, MD). Acetone, acetonitrile (HPLC grade), ampicillin sodium salt, chloroform, glycerol, sodium phosphate (monobasic), sodium phosphate (dibasic), sulfuric acid, Tris base (trishydroxymethylaminomethane), and water (HPLC grade) were purchased from Fisher Chemical (Fair Lawn, NJ). Hydrochloric acid and sodium chloride were purchased from J. T. Baker (Phillipsburg, NJ). Non-fat dry milk and Tween 20 were purchased from BioRad (Hercules, CA). Bleach was purchased from James Austin Co. (Mars, PA). Deionized water (ddH2O, 18 MΩ·cm, Milli-Q) and PBS (dissolved in de-ionized water) were autoclaved before use.

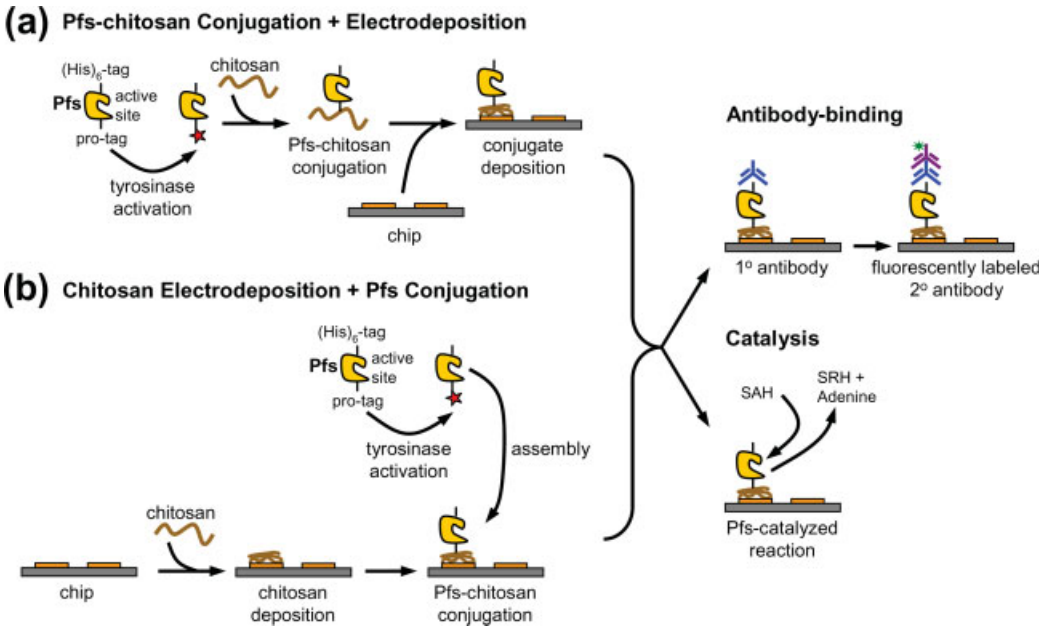

Scheme 2. **(a) Pfs-chitosan conjugation followed by electrodeposition. First, Pfs was conjugated to chitosan in solution upon tyrosinase activation of the pro-tag. Then, the Pfs-chitosan conjugate was electrodeposited onto a chip. (b) Chitosan electrodeposition followed by Pfs-chitosan conjugation. First, chitosan scaffold was electrodeposited onto a chip. Then, Pfs was assembled from solution onto the scaffold upon tyrosinase activation of the pro-tag. In both (a) and (b), the assembled Pfs bound fluorescently labeled antibody or catalyzed SAH cleavage into SRH + Adenine.**

Plasmid construction

pTrcHis-Pfs-Tyr plasmid construction was reported previously.[32] Briefly, the plasmid was constructed by PCR amplification of *pfs* from *E. coli* wild type strain W3110. Following digestion, the PCR products were extracted by gel purification and inserted into pTrcHisC (Invitrogen). DNA sequencing was performed to verify construct integrity. The plasmid was transformed into *E. coli* DH5α (defective *luxS* strain).

Purification of (His)$_6$-Pfs-(Tyr)$_5$

E. coli DH5α containing pTrcHis-Pfs-Tyr was cultured at 37°C and 250 rpm in LB medium supplemented with ampicillin at 50 μg/mL. When the OD_{600nm} reached 0.5–0.6, IPTG was added to induce enzyme production at a final concentration of 1 mM IPTG. After an additional 5 h, the culture was centrifuged for 10 min at 10,000*g*, and the cell pellet stored at −20°C. The thawed pellet was resuspended in PBS + 10 mM imidazole, pH 7.5, placed in an ice-water bath, and the cells lysed by sonication (Fisher Scientific Sonic Dismembrator 550). The lysed cells were centrifuged for 10 min 16,000*g* to remove insoluble cell debris, and the supernatant filtered through 0.22-μm PES filter. The enzyme was purified from the filtered soluble cell extract by immobilized metal-ion affinity chromatography (IMAC) using a 5 mL HisTrap chelating column (Amersham Biosciences). Before loading the filtered extract, the column was charged with Ni^{2+} ions using 0.1 M $NiSO_4$, washed with deionized water, and equilibrated with 3 column volumes (CVs) of 20 mM sodium phosphate, 250 mM NaCl, 10 mM imidazole, pH 7.4. After loading the filtered extract, the column was washed with 3 CVs of the previous buffer, washed again with 3 CVs of 20 mM sodium phosphate, 250 mM NaCl, 50 mM imidazole, pH 7.4, and the protein was eluted using 1.5 CVs of 20 mM sodium phosphate, 250 mM NaCl, 350 mM imidazole, pH 7.4. All steps were performed at 2 mL/min (1 cm/min linear velocity). The eluted sample was dialyzed overnight (16 h) at 4°C into PBS. Purified protein concentration was determined with a UV/vis spectrophotometer (DU 640, Beckman, Fullerton, CA) using UV light at 280 nm wavelength. The protein solution was mixed 2 : 1 with glycerol, alliquoted, and stored at –80°C.

Chitosan preparation

Chitosan solution was prepared by adding chitosan flakes in deionized water, with HCl added dropwise to maintain pH ~ 2, and mixing overnight. The pH was then adjusted to 3.6 by adding 1 M NaOH dropwise, and the chitosan solution was then filtered and stored at 4°C until use.

Chip fabrication

The microfabrication process for the chips was reported previously.[33] Briefly, 4′ diameter silicon wafers were coated with 1 μm silicon nitride film, followed by deposition of 50 Å chromium film, and finally, deposition of 2000 Å gold film. The patterns were created by photolithography, and the photoresist removed using acetone. The chips contain two upper gold rectangular patterns (6 mm long × 3 mm wide). The left upper pattern was where the alligator clip was attached. The upper patterns are each linked by 8-mm gold lines to two lower gold rectangular patterns (8 mm long). The left lower patterns are 0.2, 0.5, 1, 2, and 4 mm wide. The right lower patterns are all 1 mm wide. The left lower pattern was where the assembly was performed. Before the start of every experiment, each chip was cleaned by incubation in 1.4 M HCl for 30 min, followed by incubation in concentrated bleach for 20 min.

Pfs-chitosan conjugation and chip assembly

First, the chip was incubated in 1% (w/v) BSA–PBS for 2 h, rinsed with deionized water, and set aside. The conjugate was prepared by incubating $(His)_6$-Pfs-$(Tyr)_5$ (0.2 mg/mL), tyrosinase (0.1 mg/mL or 166 U/mL), and chitosan (0.5 % (w/w)) in 50 mM sodium phosphate buffer (final pH of mixture 6.0) for 2 h at 30°C and 250 rpm, followed by incubation in sodium cyanoborohydride (0.2 mg/mL) for 15 min at room temperature and 250 rpm. The conjugate was deposited onto the left gold electrode pattern by dipping the chip into the conjugate until the pattern was submerged and applying negative bias to the pattern (2 min at 2.5 A/m^2). This was done by connecting the cathode and anode (nickel chromium wire) using alligator clips to a DC power supply (Keithley 2400 SourceMeter). After deposition, the chip was rinsed with deionized water. For antibody-binding experiments, the chip was incubated in 5% nonfat dry milk–PBS for 4 h, rinsed with deionized water, and washed with gentle shaking 3 × 5 min in 5 mL TTBS (20 mM Tris-HCl, 500 mM NaCl, 0.05% (v/v) Tween-20, pH 7.5) followed by antibody incubation. For determining catalytic activity of assembed conjugate, the chip was washed with gentle shaking 3 × 5 min in 5 mL TTBS and 3 × 5 min in 5 mL TBS, and then incubated for 8 h at 37°C in 1 mL of 1 mM SAH. At reaction time points, samples were taken and immediately extracted with chloroform to stop the reaction, and the extracted samples were stored at –20°C before injecting on the HPLC.

Pfs activation and assembly onto scaffold of chip

Chitosan scaffold was deposited onto the left gold electrode pattern by dipping the chip into chitosan solution (0.5 % (w/w), pH 3.7) until the pattern was submerged and applied negative bias to the pattern (2 min at 16 A/m^2). After deposition, the chip was rinsed with deionized water and then with PBS. It was incubated in 5% (w/v) nonfat dry milk–PBS for 4 h, followed by incubation in both tyrosinase (0.1 mg/mL or 166 U/mL) and $(His)_6$-Pfs-$(Tyr)_5$ (0.1 mg/mL) in PBS for 16 h at 4°C. It was then incubated in sodium cyanoborohydride (0.2 mg/mL) in deionized water for 15 min, rinsed with deionized water, and washed with gentle shaking 3 × 5 min in 5 mL TTBS. In the antibody-binding experiments, two controls were also performed: (1) chip with assembled scaffold incubated in $(His)_6$-Pfs-$(Tyr)_5$ (0.1 mg/mL) only (no tyrosinase), and (2) chip with assembled scaffold not incubated in $(His)_6$-Pfs-$(Tyr)_5$ or tyrosinase. For all antibody-binding experiments, following TTBS washes the chip was incubated in antibody solution. For determining catalytic activity of assembled Pfs, following TTBS washes the chip was further washed 3 × 5 min in 5 mL TBS, and then was incubated for 8 h at 37°C in 1 mL of 1 mM SAH. For determining Michaelis-Menten kinetics, following TTBS washes the chip was further washed 3 × 5 min in 5 mL TBS. It was then incubated for 1 h at 37°C 225 rpm in 1 mL each of 1 mM, 0.25 mM, and 0.1 mM SAH. All reaction samples were immediately extracted with chloroform to stop the reactions, and the extracted samples were stored at –20°C before injecting on the HPLC.

Antibody binding to assembled Pfs

Following TTBS washes, the chip was incubated 1 h in 1 : 100 mouse anti-poly-histidine in 1% (w/v) nonfat dry milk–TTBS, and washed 3 × 5 min in 5 mL TTBS. It was then incubated 1 h in 1 : 100 goat anti-mouse IgG FITC-conjugated in 1% (w/v) nonfat dry milk–TTBS. Finally, it was washed with gentle shaking 3 × 5 min in 5 mL TTBS and 3 × 5 min in 5 mL TBS (20 mM Tris-HCl, 500 mM NaCl, pH 7.5) before viewing under the fluorescence microscope. ImageJ software (National Institutes of Health) was used to analyze fluorescence intensities of fluorescence micrographs.

HPLC analysis of Pfs reaction samples

A Waters Spherisorb Silica column (250 × 4.6 mm) with 5 μm beads (80 Å pore) was used in reversed-phase mode with 5 μL sample injection size and a mobile phase of 70 : 30 acetonitrile:water at 0.5 mL/min. Conversion was calculated from elution data at 210 nm. The HPLC system consisted of two Dynamax model SD-200 pumps (with 10 mL pump heads and mixing valve) and a Dynamax Absorbance Detector model UV-D II, and data was analyzed using Star 5.5 Chromatography Software (Rainin).

Results

Electrodeposition of enzyme-chitosan conjugate

We demonstrate patterned enzyme assembly onto a microfabricated chip via electrodeposition of the enzyme-chitosan conjugate onto a selected target electrode pattern, shown schematically in Figure 1a. For this, we first covalently conjugated Pfs enzyme to chitosan by incubating $(His)_6$-Pfs-$(Tyr)_5$ and tyrosinase in chitosan solution, with chitosan in excess of available Pfs to ensure all available Pfs was conjugated. Tyrosinase activates the tyrosine residues in the C-terminal pentatyrosine pro-tag to covalently link Pfs to the amines of the chitosan in solution. We then electrodeposited the Pfs-chitosan conjugate onto the target (left) gold electrode pattern (8 mm^2) by dipping the chip into the Pfs-conjugate solution until the pattern was submerged and applied negative bias to the pattern for 2 min at a constant current density of 2.5 A/m^2. This chip had been previously incubated in BSA–PBS solution to block nonspecific binding of Pfs-chitosan conjugate to the chip surfaces. It should be noted that the same Pfs-chitosan conjugate solution was repeatedly used to assemble Pfs onto multiple chips, and the chips were reused by simply cleaning in dilute hydrochloric acid followed by concentrated bleach.

We first demonstrate that Pfs-chitosan conjugate electrodeposits onto the target electrode pattern. For this, the chip with electrodeposited Pfs-chitosan conjugate was incubated in milk–PBS solution, thoroughly washed, and incubated in mouse anti-poly-histidine (1° antibody) and then in fluorescently labeled goat anti-mouse IgG (2° antibody). Milk was used to block nonspecific binding of the antibodies to the conjugate and the chip surfaces. Shown in Figure 1b are fluorescence micrographs of the target (left) electrode pattern and the right electrode pattern of the same chip with the corresponding fluorescence intensities as determined by ImageJ analysis. The fluorescence micrographs illustrate: (1) electrodeposition of the Pfs-chitosan conjugate onto the target electrode, (2) negligible binding to the silicon oxide surfaces surrounding the electrodes, and (3) significantly less binding to the other (right) electrode (44% fluorescence intensity). Overall, these results demonstrate patterned assembly of Pfs onto the chip, as the Pfs-chitosan conjugate predominately assembles onto the target electrode pattern of the chip and does not assemble onto the silicon oxide surfaces. More

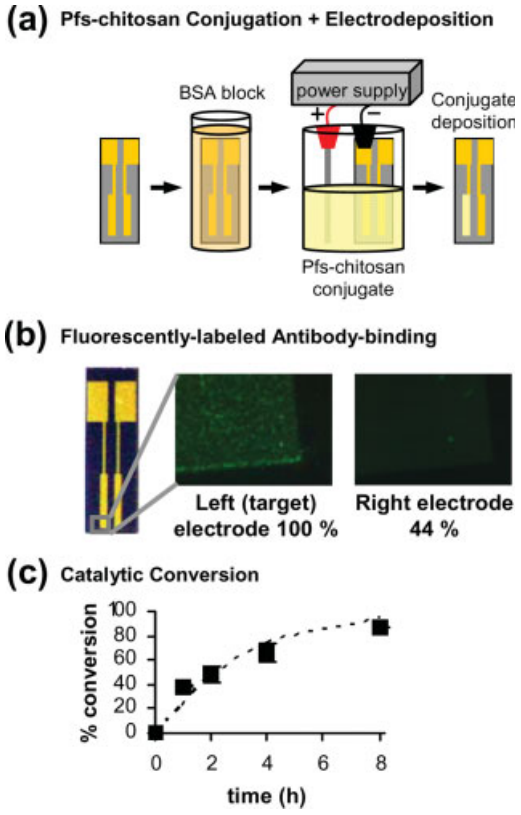

Figure 1. Electrodeposition of Pfs-chitosan conjugate.

(a) First, Pfs was conjugated to chitosan in solution upon tyrosinase-activation of the pro-tag. Then, the conjugate was electrodeposited onto the left (target) electrode (8 mm^2) of a chip that was previously blocked with BSA. (b) Fluorescence micrographs demonstrate binding of a fluorescently labeled antibody to assembled Pfs. Percentages indicate relative fluorescence intensities. (c) % catalytic conversion by assembled Pfs averaged over 2 different chips (squares), and theoretical % conversion, calculated from Michaelis-Menten saturation kinetics model (dotted line).

importantly, we demonstrate that assembled Pfs retains the necessary structure and accessibility for antibody recognition and binding.

Next, we demonstrate catalytic activity of chip-assembled Pfs-chitosan conjugate by measuring its conversion of SAH substrate into products. For this, the chip with electrodeposited Pfs-chitosan conjugate was thoroughly washed and incubated for 8 h in 1 mM SAH at 37°C. Samples were taken at regular intervals, immediately extracted with chloroform to stop the reaction, and analyzed via HPLC. Shown in Figure 1c is a plot of % SAH catalytic conversion vs. reaction time (squares), where % conversion was calculated as the % decrease in SAH concentration. Error bars (standard deviations) were calculated by repeating the experiment twice on different days with different chips and different batches of Pfs and tyrosinase, and demonstrate the reproducibility of conversion at each time point. A V_m (maximum reaction rate) of 0.38 mM/h was calculated as the initial reaction rate at 1 h, wherein the initial rate was linear. Also shown is a plot of the theoretical % conversion vs. time (dotted line), calculated from the Michaelis-Menten saturation kinetics model for a batch reactor. For this, the experimentally determined V_m of 0.38 mM/h was entered into the model, along with a K_m constant of 0.75 mM, a value which allowed for a best-fit of the calculated substrate concentrations with the experimental concentrations. Figure 1c demonstrates that assembled Pfs retained its catalytic activity throughout both the conjugation and electrodeposition steps, as SAH substrate was converted into enzymatic reaction products. Importantly, this indicates retention of its active site conformation, its overall 3-dimensional structure, and its accessibility to the substrate. Figure 1c also demonstrates that the catalytic conversion of SAH by assembled Pfs follows the Michaelis-Menten kinetic model.

In summary, Figure 1 demonstrates a technique for patterned assembly of active enzyme onto a microfabricated chip. The target enzyme is first covalently conjugated to chitosan upon activation of the pro-tag, and the conjugate is then electrodeposited onto a patterned electrode. The assembled enzyme remains accessible for antibody recognition and binding, and retains reproducible catalytic activity.

Enzyme conjugation to electrodeposited chitosan scaffold

Next, we demonstrate patterned enzyme assembly onto a microfabricated chip via covalent conjugation of the enzyme to an already electrodeposited chitosan scaffold pattern, shown schematically in Figure 2a. For this, we first electrodeposited chitosan scaffold onto the target (left) gold electrode pattern (8 mm^2) by dipping the chip in chitosan solution until the pattern was submerged and applied negative bias to the pattern for 2 min at a constant current density of 16 A/m^2. The chip was then incubated in milk–PBS solution to block nonspecific binding of Pfs to chitosan and the chip surfaces. Next, the chip was incubated in a PBS solution containing $(His)_6$-Pfs-$(Tyr)_5$ and tyrosinase. Tyrosinase activates the pro-tag to covalently link Pfs to the amines of the patterned chitosan scaffold. Finally, the chip was thoroughly washed.

We first demonstrate that tyrosinase-activated Pfs is assembled only onto the patterned scaffold. For this, the chip was incubated in mouse anti-poly-histidine (1° antibody) and then in fluorescently labeled goat anti-mouse IgG (2° antibody). Shown in Figure 2b are fluorescence micrographs with the corresponding fluorescence intensities as determined by ImageJ analysis. The first micrograph ("+ tyrosinase + Pfs") illustrates that Pfs assembled only onto the patterned scaffold, and that nonspecific binding of Pfs to the other chip surfaces was negligible, as there is no discernable fluorescence on the right gold electrode pattern or the silicon oxide. The strong fluorescence intensity illustrates significant antibody binding. The second micrograph ("– tyrosinase + Pfs") represents a negative control, where the chip with patterned scaffold was incubated in $(His)_6$-Pfs-$(Tyr)_5$ alone (no tyrosinase activation). This chip yielded significantly less fluorescence (13% fluorescence intensity based on ImageJ analysis), indicating minimal nonspecific binding of Pfs to the patterned scaffold, and that tyrosinase activation is required for Pfs assembly. Thus, tyrosinase-activated Pfs assembles covalently onto the scaffold. The third micrograph ("– tyrosinase – Pfs") represents a second control, where the chip with patterned scaffold was not incubated in Pfs or tyrosinase. This chip yielded even less fluorescence (6% fluorescence intensity based on ImageJ analysis), indicating minimal nonspecific binding of the antibodies to the patterned scaffold. Overall, Figure 2b demonstrates patterned and covalent assembly of Pfs onto the chip, as Pfs assembles only onto the patterned scaffold, and as tyrosinase activation is required for Pfs assembly. Additionally, Figure 2b

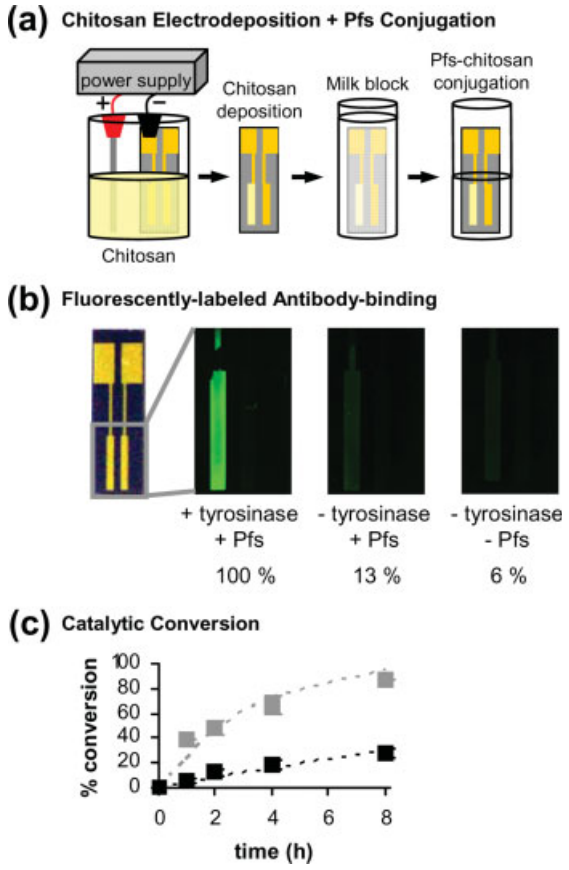

Figure 2. Pfs conjugation to electrodeposited chitosan scaffold.

(a) First, chitosan scaffold was electrodeposited onto the left (target) electrode (8 mm^2) of a chip. Chip was blocked with milk. Then, Pfs was conjugated to the scaffold upon tyrosinase-activation of the pro-tag. (b) Fluorescence micrographs demonstrate binding of a fluorescently labeled antibody to assembled Pfs. Percentages indicate relative fluorescence intensities. (c) % catalytic conversion by assembled Pfs averaged over six different chips (black squares), and theoretical % conversion, calculated from Michaelis-Menten saturation kinetics model (black dotted line). Shown in gray are previous data from Figure 1c.

demonstrates that assembled Pfs retained the necessary structure and accessibility for antibody recognition and binding.

Next, we demonstrate catalytic activity of assembled Pfs by measuring its conversion of SAH substrate into products. For this, the chip was incubated for 8 h in 1 mM SAH at 37°C. Samples were taken at regular intervals, immediately extracted with chloroform to stop the reaction, and analyzed via HPLC. Shown in Figure 2c is a plot of % SAH substrate conversion vs. reaction time (black squares), where % conversion was calculated as the % decrease in SAH concentration. Figure 2c demonstrates that the assembled Pfs retained its catalytic activity, indicating retention of its active site conformation, its overall 3-dimensional structure, and its accessibility to the substrate. Error bars (standard deviations) were calculated by repeating the experiment six times on different days with six different chips and using multiple batches of Pfs, tyrosinase, and SAH. The error bars demonstrate the high level of control of our assembly approach, as conversion is reproducible at each reaction time point. A V_m (maximum reaction rate) of 0.06 mM/h was calculated as the initial reaction rate at 1 h for these experiments. Also shown is a plot of the theoretical % conversion vs. time (black dotted line), calculated from the Michaelis-Menten model for a batch reactor. For this, the experimentally determined V_m of

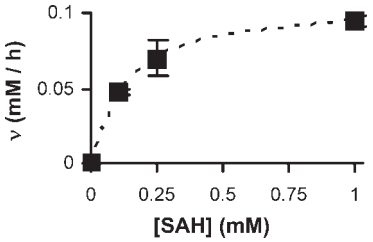

Figure 3. Rate of SAH conversion by assembled Pfs (squares) follows Michaelis-Menten saturation kinetics model (dotted line).

Pfs assembled by conjugation to electrodeposited chitosan scaffold.

0.06 mM/h was entered into the model, along with a K_m constant of 0.75 mM, a value which allowed for a best-fit of the calculated substrate concentrations with the experimental concentrations. This demonstrates that the catalytic conversion of SAH by assembled Pfs follows the Michaelis-Menten kinetics model. Finally, shown in gray are the previous data from Figure 1c, demonstrating more conversion when Pfs assembly occurred via electrodeposition of Pfs-chitosan conjugate vs. Pfs conjugation to electrodeposited chitosan. Further analysis revealed that this was entirely due to differences in the overall amount of Pfs assembled (V_m was different between Figures 1c and 2c due to enzyme level, not maximum rate). Information on quantification of Pfs assembly can be found in the Supplemental Information section.

In summary, Figure 2 demonstrates a second technique for patterned assembly of active enzyme onto a microfabricated chip. The chitosan scaffold is first electrodeposited onto a patterned electrode, and then the target enzyme is covalently conjugated to the patterned scaffold upon activation of the pro-tag. The assembled enzyme remains accessible for antibody recognition and binding, and retains reproducible catalytic activity.

Kinetics of substrate catalytic conversion by assembled enzyme

Next, we examine the reaction kinetics of SAH substrate conversion by assembled Pfs enzyme by performing initial rate experiments. For this, we first electrodeposited chitosan scaffold onto the target (left) gold electrode pattern (8 mm^2) by dipping the chip in chitosan solution until the pattern was submerged and applied negative bias to the pattern for 2 min at a constant current density of 16 A/m^2. The chip was then incubated in milk–PBS solution to block nonspecific binding of Pfs to chitosan and the chip surfaces. Next, Pfs was covalently assembled onto the scaffold by incubating the chip in a PBS solution containing $(His)_6$-Pfs-$(Tyr)_5$ and tyrosinase. After thoroughly washing the chip, it was incubated for 1 h at 37°C with thorough mixing in SAH concentrations of 1 mM, 0.25 mM, and 0.1 mM. Samples were taken at regular intervals, immediately extracted with chloroform to stop the reaction, and analyzed via HPLC.

Shown in Figure 3 is a plot of initial reaction rate (v, in mM/h) vs. initial SAH substrate concentration ([SAH], in mM). Error bars (standard deviations) were calculated by repeating the experiment three times on different days with three different chips, demonstrating that the rate of catalytic conversion is reproducible for a given substrate concentration. This plot demonstrates that the catalytic conversion of

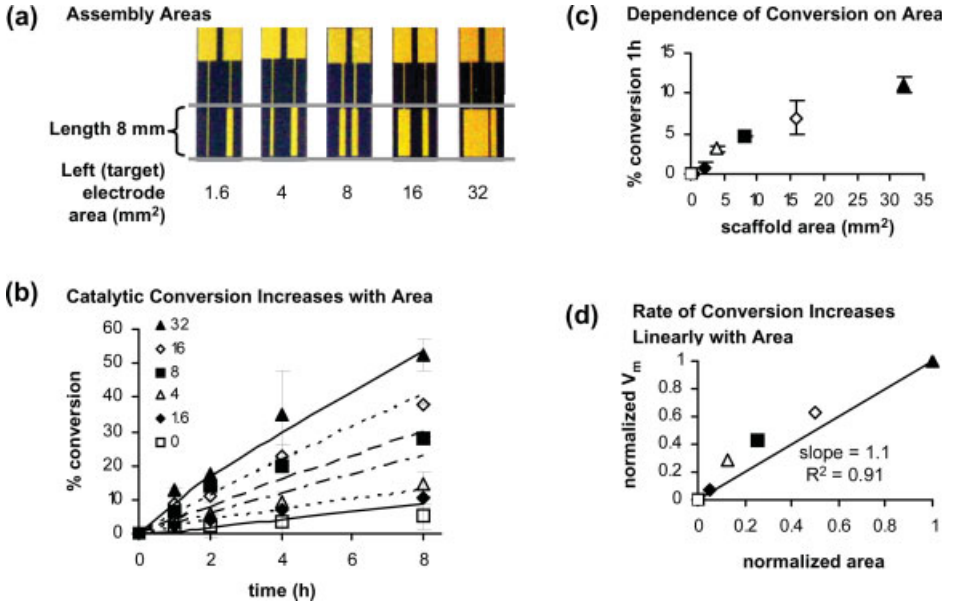

Figure 4. SAH conversion by assembled Pfs linearly correlates with assembly area.

(a) Increasing assembly areas. (b) % catalytic conversion of SAH by assembled Pfs. Legend indicates assembly area (mm^2). The data for 0 mm^2 represents the % conversion by Pfs assembled nonspecifically onto the chip surfaces. (c) % catalytic conversion of SAH at 1h for a given assembly area, where the [SAH] converted by the non-specifically assembled Pfs has not been included. (d) Maximum rate of SAH conversion (V_m, in mM/h) for a given assembly area, calculated from data in Figure 4c, where V_m and area have been normalized against the maximum values.

SAH by assembled Pfs follows Michaelis-Menten saturation kinetics. A K_m constant of 0.12 ± 0.04 mM and a V_m of 0.11 ± 0.02 mM/h (maximum rate of conversion) were calculated via Lineweaver-Burk method. This V_m corresponds to 1.8 nanomoles per minute for a 1 mL reaction solution volume. We note that the K_m here is less than that determined previously for the data in Figures 1c and 2c (0.75 mM), which may be due to decreased mass transfer limitations here, as the reaction solutions were well-mixed. The dashed line in Figure 3d is a plot of v vs. [SAH], where v was calculated from the Michaelis-Menten rate expression, $v = V_m \cdot [SAH]/(K_m + [SAH])$, using our values of K_m and V_m. As shown, the kinetic model agrees well with our experimental values. Overall, Figure 3 demonstrates that our assembly approach allows for examination of in vitro enzymatic reaction kinetics in a reproducible manner.

Area-based manipulation of substrate conversion

Finally, we demonstrate that substrate conversion is user-manipulated via the assembly area. That is, by modulating the assembly area, and hence, the amount of Pfs assembly, SAH conversion is correspondingly modulated. For this, we first electrodeposited chitosan scaffolds onto microfabricated chips with increasing areas of the target (left) gold electrode patterns. Shown in Figure 4a, these chips have target electrode patterns of increasing areas of 1.6, 4, 8, 16, and 32 mm^2, respectively. Electrodeposition was performed for each chip by dipping in chitosan solution until the pattern was submerged and applied negative bias to the pattern for 2 min at a constant current density of 16 A/m^2, creating chitosan scaffolds of the same patterned areas as the corresponding electrodes. These chips were then incubated in milk–PBS solution to block nonspecific binding of Pfs to chitosan and the chip surfaces. Next, Pfs was covalently assembled onto the scaffolds by incubating the chips in $(His)_6$-Pfs-$(Tyr)_5$ and tyrosinase. Additionally, we examined nonspecific assembly of Pfs onto the chip surfaces (gold and silicon oxide) by performing a negative control, where a chip without electrodeposited chitosan scaffold was incubated in milk–PBS, and then incubated in $(His)_6$-Pfs-$(Tyr)_5$ alone (without tyrosinase). After thorough washing, the chips were each incubated for 8 h in 1 mL of 1 mM SAH at 37°C. Samples were taken at regular intervals, immediately extracted with chloroform to stop the reaction, and analyzed via HPLC.

Shown in Figure 4b is a plot of % SAH substrate catalytic conversion vs. reaction time for each patterned scaffold area (points), with each point representing the average of two separate experiments performed with two different chips. There is a baseline level of nonspecific Pfs assembly onto the chip surfaces (gold and silicon oxide), as demonstrated by the % conversion for 0 mm^2 scaffold area. This plot demonstrates that SAH conversion increases with assembly area, and that our assembly approach is highly controlled, as SAH conversion is reproducible for each area and each time point. Also shown is a plot of the theoretical % conversion vs. time for each patterned area (lines), calculated from the Michaelis-Menten saturation kinetics model for a batch reactor. For this, the experimentally determined V_m for each area was entered into the model, along with a K_m constant of 0.75 mM, a value which allowed for a best-fit of the calculated substrate concentrations with the experimental concentrations. These calculations show that the experimentally measured SAH conversion for each assembly area follows the Michaelis-Menten model.

Shown in Figure 4c is a plot of % SAH catalytic conversion at 1 h vs. scaffold area (in mm^2). For this, the SAH converted by the non-specifically assembled Pfs was not included, i.e. was subtracted from the total SAH converted for each area. Using this data shown in Figure 4c, a corrected initial rate of conversion for each area was calculated, i.e. corrected V_m: 0.0084, 0.031, 0.046, 0.069, and 0.11 mM/h

for 1.6, 4, 8, 16, and 32 mm^2, respectively. Shown in Figure 4d is a plot of corrected V_m vs. scaffold area (in mm^2), where V_m and area have been normalized against their corresponding maximum values. As shown, the rate of conversion increases linearly with area. More importantly, as the line drawn through the normalized data indicates a doubling of area results in a doubling of the rate of conversion. A linear regression through the data resulted in a slope of 1.1 ($R^2 = 0.91$). Further analysis revealed that this was due entirely due to the Pfs assembly, i.e. a doubling of area resulted in a doubling of mg Pfs assembled. Information on quantification of Pfs assembly can be found in the Supplemental Information section. Combined, Figures 4c, d demonstrate that the end-user can predict the conversion based on the assembly area, allowing for control of conversion through manipulation of the assembly area, i.e. area-based manipulation of conversion.

In summary, Figure 4 demonstrates that the rate of catalytic conversion by assembled enzyme is reproducible for a given assembly area, allowing for area-based manipulation of conversion. As the enzyme is assembled onto pre-fabricated devices, this is accomplished simply by varying the scaffold assembly process (i.e. electrodeposition).

Discussion

We report an approach for active enzyme assembly onto microfabricated chip surfaces based on the electrodeposition of chitosan onto selected electrodes of the chips and the covalent conjugation of the target enzyme (in this case, Pfs) to chitosan upon biochemical activation of a C-terminal protag. Using this approach, there are two possible methodologies, as shown in Scheme 2. In the first method (Scheme 2a), the target enzyme is first covalently conjugated to chitosan, and this conjugate is then electrodeposited onto a selected electrode. In the second method (Scheme 2b), chitosan is first electrodeposited onto a selected electrode, and the target enzyme is then covalently conjugated to the electrodeposited chitosan. These methods are interchangeable in that they both assemble active enzyme in a spatially selective manner. However, there are some differences, as demonstrated by comparison of Figure 1 (conjugation then electrodeposition) to Figure 2 (electrodeposition then conjugation).

One difference in the two methods is the level of binding of fluorescently labeled antibody to assembled Pfs, observed by comparing the fluorescence intensities of the micrographs of the left (target) electrodes in Figures 1b and 2b, which were identically prepared. The micrograph in Figure 1b displays 21% of the fluorescence intensity of the micrograph in Figure 2b, indicating less antibody binding. We believe this is due to the accessibility of assembled Pfs for antibody binding. In the first method, the electrodeposited conjugate film contains Pfs imbedded within the film as well as Pfs displayed on the surface of the film, and additionally, this surface-displayed Pfs may not be in any particular orientation with respect to the film surface. Thus, the Pfs assembled by the first method is expected to be less accessible for antibody binding, which is consistent with the weak fluorescence intensity of Figure 1b. In the second method, the Pfs predominately conjugates to the surface of the electrodeposited chitosan film, as Pfs is presented after chitosan deposition, and as diffusion of Pfs into the film is presumably limited due to steric hindrance effects. Additionally, Pfs preferentially conjugates to chitosan film through its C-terminal protag vs. its native tyrosines,[34] indicating that Pfs is preferentially oriented through the pro-tag with respect to the film surface. Thus, the Pfs assembled by the second method is expected to be more accessible for antibody binding, which is consistent with the strong fluorescence intensity of Figure 2b. Combined, the antibody-binding results of Figures 1b and 2b indicate that the second assembly method (electrodeposition then conjugation) could be more appealing for applications involving protein–protein recognition and protein–protein binding. However, the data clearly demonstrates that both methods assemble enzymes that can recognize and bind antibodies.

Another difference in the two methods is the catalytic conversion of SAH substrate by assembled Pfs, observed by comparing % conversion at each time point in Figures 1c and 2c. Significantly higher conversion is observed when Pfs is assembled by the first method (conjugation then electrodeposition) vs. the second method (electrodeposition then conjugation) (86% vs. 27% at 8 h). Further analysis revealed this was entirely due to differences in the amount of Pfs assembled by each method, rather than differences in Pfs stability or activity. Information on quantification of Pfs assembly can be found in the Supplemental Information section. In fact, Pfs is stabilized by chitosan-conjugation and additionally by device-assembly, allowing for increased activity over extended periods of time.[35] Nonetheless, the high conversion observed in Figure 1c strongly suggests that diffusion of small molecules (e.g. SAH) is possible within the electrodeposited chitosan film. Importantly, the data clearly demonstrates that both methods assemble enzymes that retain catalytic activity.

Our assembly approach allowed for controlled examination of enzymatic catalysis and kinetics. Specifically, we examined the kinetics of SAH catalytic conversion by assembled Pfs, where Pfs was assembled by the second method (conjugation then electrodeposition), and where the reaction solutions were well-mixed. We report that this reaction follows Michaelis-Menten saturation kinetics with a K_m constant of 0.12 ± 0.04 mM. Reported values of the Michaelis-Menten constant K_m have varied widely.[21,29] Duerre [21] reports a K_m of 3 mM, while Ragione et al.[29] report a K_m of 4.3 μM. This discrepancy in K_m values is attributed by Ragione et al. to differences in enzyme purity and in the assay used to determine conversion; we also have used different purification and analytical techniques. Additionally, higher K_m constants for immobilized enzymes compared with free enzymes in solution has been reported.[4,9] This is generally attributed to steric hindrance effects and mass transfer limitations associated with immobilized enzymes vs. free enzymes in solution. The higher K_m of 0.75 mM determined for Figures 1c, 2c, and 4b may also be due to increased mass transfer limitations, as for these experiments, the reactions solutions were not mixed. Nonetheless, our values of K_m are well within the range of reported values of K_m.

The two methods of our overall assembly approach both allow for user-controllable patterned assembly of active enzymes onto microfabricated chips, and are appealing for a variety of potential applications. In particular, we envision using the first method (conjugation then electrodeposition) to pattern multiple enzymes onto the same chip, where each enzyme-chitosan conjugate would be sequentially electrodeposited onto its own distinct electrode pattern of a single chip. The electrode patterns (assembly areas) could be different for each enzyme, thus allowing for simultaneous in vitro examination and manipulation of multiple-step enzymatic

reactions in a controlled manner. The results reported here extend our previous reports on the assembly of proteins onto patterned surfaces. In particular, we have previously shown the conjugation of a marker protein (GFP) onto already electrodeposited chitosan films[36]; we have also demonstrated the sequential assembly of multiple proteins[37] via the activation of electrodeposited chitosan using a glutaraldehyde treatment. Finally, we have also demonstrated the electrodeposition of a marker protein/chitosan conjugate.[37] The present scenarios, which employ enzymatic activation for the assembly of enzymes, expand the repertoire of methods for "biofunctionalization" (postfabricated assembly) of devices.

Conclusions

Our results demonstrate patterned assembly of Pfs enzyme fused with a C-terminal pentatyrosine pro-tag. Equally important, they demonstrate that the assembled enzyme retains its biocatalytic activity for small molecule biosynthesis and its accessibility for antibody binding. Moreover, the rate of biocatalysis is reproducible for a particular assembly area, allowing for controlled examination of enzymatic reaction kinetics, and area-based manipulation of the rate of biocatalysis and small molecule biosynthesis, thus enabling optimization of biosynthesis in 1-step as well as multistep enzymatic reactions. We are currently using our approach to screen Pfs inhibitors in the search for novel antibiotics and we envision in vitro metabolic engineering applications based on optimizing catalysis in entire metabolic pathways.

Acknowledgments

This work was supported in part by the Robert W. Deutsch Foundation and the Natural Science Foundation (#EFRI-735987).

Literature Cited

1. Norde W. Adsorption of proteins from solution at the solid-liquid interface. *Adv Colloid Interface Sci*. 1986;25:267–340.
2. Wessa T, Rapp M, Sigrist H. Immunosensing of photoimmobilized proteins on surface acoustic wave sensors. *Colloids Surf B*. 1999;15:139–146.
3. Zhen G, Eggli, V, Voros J, Zammaretti P, Textor M, Glockshuber R, Kuennemann E. Immobilization of the enzyme β-lactamase on biotin-derivatized poly(L-lysine)-*g*-poly(ethylene glycol)-coated sensor chips: a study on oriented attachment and surface activity by enzyme kinetics and in situ optical sensing. *Langmuir*. 2004;20:10464–10473.
4. Xu F, Zhen GL, Yu F, Kuennemann E, Textor M, Knoll W. Combined affinity and catalytic biosensor: in situ enzymatic activity monitoring of surface-bound enzymes. *J Am Chem Soc*. 2005;127:13084–13085.
5. Cosnier S, Molins C, Mousty C, Galland B, Lepellec A. A simple strategy based on photobiotin irradiation for the photoelectrochernical immobilization of proteins on electrode surfaces. *Mater Sci Eng C*. 2006;26:436–441.
6. Miao Y, Tan SN. Amperometric hydrogen peroxide biosensor with silica sol-gel/chitosan film as immobilization matrix. *Anal Chim Acta*. 2001;437:87–93.
7. Chen X, Jia JB, Dong SJ. Organically modified sol-gel/chitosan composite based glucose biosensor. *Electroanalysis*. 2003;15:608–612.
8. Wang G, Xu JJ, Chen HY, Lu ZH. Amperometric hydrogen peroxide biosensor with sol-gel/chitosan network-like film as immobilization matrix. *Biosens Bioelectron*. 2003;18:335–343.
9. Sung WJ, Bae YH. Glucose oxidase, lactate oxidase, and galactose oxidase enzyme electrode based on polypyrrole with polyanion/PEG/enzyme conjugate dopant. *Sens Actuators B Chem*. 2006;114:164–169.
10. WuLQ, Gadre AP, Yi HM, Kastantin MJ, Rubloff GW, Bentley WE, Payne GF, Ghodssi, R. Voltage-dependent assembly of the polysaccharide chitosan onto an electrode surface. *Langmuir*. 2002;18:8620–8625.
11. Wu LQ, Yi HM, Li S, Rubloff GW, Bentley WE, Ghodssi R, Payne GF. Spatially selective deposition of a reactive polysaccharide layer onto a patterned template. *Langmuir*. 2003;19:519–524.
12. Wu LQ, Payne GF. Biofabrication: using biological materials and biocatalysts to construct nanostructured assemblies. *Trends Biotechnol*. 2004;22:593–599.
13. Luo XL, Xu JJ, Du Y, Chen HY. A glucose biosensor based on chitosan-glucose oxidase-gold nanoparticles biocomposite formed by one-step electrodeposition. *Anal Biochem*. 2004;334:284–289.
14. Luo XL, Xu JJ, Zhang Q, Yang GJ, Chen HY. Electrochemically deposited chitosan hydrogel for horseradish peroxidase immobilization through gold nanoparticles self-assembly. *Biosens Bioelectron*. 2005;21:190–196.
15. Pang X, Zhitomirsky I. Electrodeposition of composite hydroxyapatite-chitosan films. *Mater Chem Phys*. 2005;94:245–251.
16. Yi HM, Wu LQ, Bentley WE, Ghodssi R, Rubloff GW, Culver JN, Payne GF. Biofabrication with chitosan. *Biomacromolecules*. 2005;6:2881–2894.
17. Chen TH, Embree HD, Wu LQ, Payne GF. In vitro protein-polysaccharide conjugation: Tyrosinase-catalyzed conjugation of gelatin and chitosan. *Biopolymers*. 2002;64:292–302.
18. Chen TH, Small DA, Wu LQ, Rubloff GW, Ghodssi R, Vazquez-Duhalt R, Bentley WE, Payne G F. Nature-inspired creation of protein-polysaccharide conjugate and its subsequent assembly onto a patterned surface. *Langmuir*. 2003;19:9382–9386.
19. Freddi G, Anghileri A, Sampaio S, Buchert J, Monti P, Taddei P. Tyrosinase-catalyzed modification of Bombyx mori silk fibroin: grafting of chitosan under heterogeneous reaction conditions. *J Biotechol*. 2006;125:281–294.
20. Sampaio S, Taddei P, Monti P, Buchert J, Freddi G. Enzymatic grafting of chitosan onto Bombyx mori silk fibroin: kinetic and IR vibrational studies. *J Biotechnol*. 2005;116:21–33.
21. Duerre JA. Hydrolytic nucleosidase acting on s-adenosylhomocysteine and on 5′-methylthioadenosine. *J Biol Chem*. 1962;237:3737–3741.
22. Miller CH, Duerre JA. S-ribosylhomocysteine cleavage enzyme from Escherichia Coli. *J Biol Chem*. 1968;243:92–97.
23. Riscoe MK, Tower PA, Ferro AJ. Mechanism of action of 5′-methylthioadenosine in S49 cells. *Biochem Pharmacol*. 1984;33:3639–3643.
24. Raina A, Tuomi K, Pajula RL. Inhibition of the synthesis of polyamines and macromolecules by 5′-methylthioadenosine and 5′-alkylthiotubercidins in Bhk-21-cells. *Biochem J*. 1982;204:697–703.
25. Pajula RL, Raina A. Methylthioadenosine, a potent inhibitor of spermine synthase from bovine brain. *FEBS Lett*. 1979;99:343–345.
26. Borchardt RT. *S*-adenosyl-L-methionine-dependent macromolecule methyltransferases: potential targets for the design of chemotherapeutic agents. *J Med Chem*. 1980;23:347–357.
27. Delahaba G, Cantoni GL. Enzymatic synthesis of *S*-adenosyl-L-homocysteine from adenosine and homocysteine. *J Biol Chem*. 1959;234:603–608.
28. Cornell KA, Swarts WE, Barry RD, Riscoe MK. Characterization of recombinant *Escherichia coli* 5′-methylthioadenosine/S-adenosylhomocysteine nucleosidase: analysis of enzymatic activity and substrate specificity. *Biochem Biophys Res Commun*. 1996;228:724–732.
29. Ragione ED, Porcelli M, Cartenifarina M, Zappia V. *Escherichia coli S*-adenosylhomocysteine/5′-methylthioadenosine nucleosidase. Purification, substrate specificity and mechanism of action. *Biochem J*. 1985;232:335–341.

30. Singh V, Evans GB, Lenz DH, Mason JM, Clinch K, Mee S, Painter GF, Tyler PC, Furneaux RH, Lee JE, Howell PL, Schramm VL. Femtomolar transition state analogue inhibitors of 5′-methylthioadenosine/*S*-adenosylhomocysteine nucleosidase from Escherichia coli. *J Biol Chem*. 2005;280:18265–18273.
31. Singh V, Shi WX, Almo SC, Evans GB, Furneaux RH, Tyler PC, Painter GF, Lenz DH, Mee S, Zheng RJ, Schramm VL. Structure and inhibition of a quorum sensing target from *Streptococcus pneumoniae*. *Biochemistry*. 2006;45:12929–12941.
32. Fernandes R, Tsao CY, Hashimoto Y, Wang L, Wood TK, Payne GF, Bentley WE. Magnetic nanofactories: localized synthesis and delivery of quorum-sensing signaling molecule autoinducer-2 to bacterial cell surfaces. *Metab Eng*. 2007;9: 228–239.
33. Yi H, Wu LQ, Ghodssi R, Rubloff GW, Payne GF, Bentley WE. A robust technique for assembly of nucleic acid hybridization chips based on electrochemically templated chitosan. *Anal Chem*. 2004;76:365–72.
34. Lewandowski AT, Small DA, Chen T, Payne GF, Bentley WE. Tyrosine-based "activatable pro-tag": enzyme-catalyzed protein capture and release. *Biotechnol Bioeng*. 2006;93:1207–1215.
35. Luo XL, Lewandowski AT, Yi H, Payne GF, Ghodssi R, Bentley WE, Rubloff GW. Programmable assembly of a metabolic pathway enzyme in a pre-packaged reusable bioMEMS device. *Lab Chip*. 2008;8:420–430.
36. Lewandowski AT, Yi H, Luo XL, Payne GF, Ghodssi R, Rubloff GW, Bentley WE. Protein assembly onto patterned microfabricated devices through enzymatic activation of fusion protag. *Biotechnol Bioeng*. 2008;99:499–507.
37. Yi H, Wu LQ, Ghodssi R, Rubloff GW, Payne GF, Bentley WE. Signal-directed sequential assembly of biomolecules on patterned surfaces. *Langmuir*. 2005;21:2104–2107.

Manuscript received Oct. 2, 2007, and revision received Apr. 2, 2008.

BTPR070348Z